HHS Public Access

Author manuscript

Stem Cells. Author manuscript; available in PMC 2015 May 13.

Published in final edited form as:

Stem Cells. 2015 January ; 33(1): 68–78. doi:10.1002/stem.1854.

Parkin Mutations Reduce the Complexity of Neuronal Processes in iPSC-derived Human Neurons

Yong Ren[a], **Houbo Jiang**[a,b], **Zhixing Hu**[a,b], **Kevin Fan**[a], **Jun Wang**[a], **Stephen Janoschka**[c], **Xiaomin Wang**[d], **Shaoyu Ge**[c], and **Jian Feng**[a,b,d]

[a]Department of Physiology and Biophysics, State University of New York at Buffalo, Buffalo, NY 14214, USA

[b]VA Western New York Healthcare System, Buffalo, NY 14215, USA

[c]Department of Neurobiology & Behavior, State University of New York at Stony Brook, Stony Brook, NY 11794, USA

[d]Department of Neurobiology, Key Laboratory for Neurodegenerative Disorders of the Ministry of Education, Beijing Institute for Brain Disorders, Capital Medical University, Beijing 100069, China

Abstract

Parkinson's disease (PD) is characterized by the degeneration of nigral dopaminergic (DA) neurons and non-DA neurons in many parts of the brain. Mutations of parkin, an E3 ubiquitin ligase that strongly binds to microtubules, are the most frequent cause of recessively inherited Parkinson's disease. The lack of robust PD phenotype in parkin knockout mice suggests a unique vulnerability of human neurons to parkin mutations. Here, we show that the complexity of neuronal processes as measured by total neurite length, number of terminals, number of branch points and Sholl analysis, was greatly reduced in induced pluripotent stem cell (iPSC)-derived TH^+ or TH^- neurons from PD patients with parkin mutations. Consistent with these, microtubule stability was significantly decreased by parkin mutations in iPSC-derived neurons. Overexpression of parkin, but not its PD-linked mutant nor GFP, restored the complexity of neuronal processes and the stability of microtubules. Consistent with these, the microtubule-depolymerizing agent colchicine mimicked the effect of parkin mutations by decreasing neurite length and complexity in control neurons while the microtubule-stabilizing drug taxol mimicked the effect of parkin overexpression by enhancing the morphology of parkin-deficient neurons. The results suggest that parkin maintains the morphological complexity of human neurons by stabilizing microtubules.

Address correspondence to: Jian Feng, Ph.D., Department of Physiology and Biophysics, State University of New York at Buffalo 124 Sherman Hall, Buffalo, NY 14214, Phone: 1-716-829-2345; Fax: 1-716-829-2699; jianfeng@buffalo.edu.

Disclosure:
The authors declare no conflict of interest.

Supplemental Information:
Supplemental Information for this article includes 5 supplementary figures.

Author Contributions:
Y.R., H.J., Z.H., K.F., J.W.: collection and/or assembly of data, data analysis and interpretation; S.J., S.G.: data analysis and interpretation; X.W.: manuscript writing, financial and administrative support; J.F.: conception and design, data analysis and interpretation, manuscript writing, financial and administrative support, and final approval of manuscript. Keywords: induced pluripotent stem cells, Parkinson's disease, parkin, dopamine, microtubule

Introduction

The locomotor symptoms of Parkinson's disease are linked to the relatively selective degeneration of nigral DA neurons, while the loss of many other types of neurons in the brain appear to contribute to the non-motor comorbidities of PD [1]. Among monogenic mutations that are linked to Parkinson's disease, mutations of the parkin gene [2] account for the most frequent cause of recessively inherited PD [3]. Parkin is an ubiquitin ligase [4] with diverse substrates and functions (e.g. [5–8]). Our previous studies have shown that parkin binds to microtubules with very high affinity [9] through strong and independent interactions mediated by each of its three RING fingers [10]. Such strong interactions stabilize microtubules [10] and enable parkin to protect against the selective toxicity of microtubule-depolymerizing agents, including the PD environmental toxin rotenone [11,12].

The complexity of neuronal processes is a prerequisite for neurons to form networks with a vast number of synaptic connections required for information processing. Nigral DA neurons have particularly elaborate axon arborization; the total length of axon arbors of a single nigral DA neuron in rat averages 46 cm [13]. Based on the scale of the human brain, it is estimated that a human nigral DA neuron may have axon arbors with an average total length of 4.6 m [14], which may give rise to the selective vulnerability of these cells in Parkinson's disease [15]. Although it is unclear what makes these axon arbors so extensive and complex, anatomical studies from PD patients show a "dying back" phenomenon, with degeneration starting in axons of nigral DA neurons [16,17]. The very different scales of human and rodent nigral DA neurons may also explain the difficulties in developing animal models that can recapitulate key features of Parkinson's disease in human patients [18]. The dramatic difference between parkin knockout mice [19] and PD patients with parkin mutations [2] has led us to generate patient-specific induced pluripotent stem cells to study the unique functions of parkin in human midbrain DA neurons [20]. Mutations of parkin do not affect the differentiation of midbrain DA neurons from iPSCs. The number of TH^+ neurons is very similarly between patient lines and control lines [20]. The iPSC-derived neurons can be maintained for very long time without any significant cell death. Parkin mutations disrupt the precision of dopaminergic transmission and increase oxidative stress induced by dopamine [20]. Using the same sets of iPSC-derived midbrain neurons, we examined the impact of parkin mutations on neuronal processes in this study.

Materials and methods

Generation and *in vitro* differentiation of iPS cells

Under the approval of Health Sciences Institutional Review Board in the State University of New York at Buffalo, the four lines of iPS cells were generated in a previous study and were differentiated to midbrain DA neurons using the same protocol [20]. Briefly, iPSC colonies were first cultured as embryoid bodies (EB) for 4 days in hESC medium with 10 μM SB431542 to enhance neural differentiation. After four more days in 20 ng ml^{-1} bFGF, the EBs were plated on matrigel-coated 6-well plates. The neuroepithelial cells (rosettes) were culture in the presence of FGF8a (20 ng ml^{-1}) and SHH (100 ng ml^{-1}) and were peeled off after 14 days from the flat peripheral cells and cultured in suspension in the presence of FGF8a (50 ng ml^{-1}) and SHH (100 ng ml^{-1}), N2 plus B27 supplements (1×) and ascorbic

acid (200 μM) for additional 14 days to form neurospheres that were patterned to a mid/hind brain fate. The neurospheres were dissociated and plated on 24-well plates precoated with polyornithine, laminin and matrigel. Trophic factors such as BDNF (20 ng ml^{-1}) and GDNF (20 ng ml^{-1}) were used to generate mature DA neurons, which were seen around 45–50 days from the start of differentiation. All experiments were done on iPSC-derived neuronal cultures differentiated for 90 days from the beginning. In some experiments, neurons were infected by sindbis virus or lentivirus for various genes around day 76.

Plasmids, viruses and antibodies

pSinRep5-palGFP construct [13] is a generous gift from Dr. Takahiro Furuta at Kyoto University. Sindbis virus for palGFP was generated using the Sindbis Expression System (Life Technologies, Carlsbad, CA, USA). Lentiviruses for GFP, FLAG-parkin, FLAG-parkin (T240R) were generated as previously described [20]. Rabbit antibody against TH was from Affinity BioReagents (Golden, CO). Mouse antibodies against α-tubulin, FLAG, and actin were purchased from Sigma (St. Louis, MO). Alexa Fluor 488 or 594-conjugated secondary antibodies against mouse or rabbit IgG were from Molecular Probes (Eugene, OR).

Immunocytochemistry and quantitative image analysis

iPSC-derived neuronal cultures in 24-well plates were fixed with 4% paraformaldehyde, permeabilized in 0.1% Triton X-100 and blocked with 5% BSA. They were incubated with primary antibodies overnight at 4°C. After the cultures were washed and incubated with fluorescent secondary antibodies for 2 hr at room temperature, they were imaged on Zeiss Axio Observer inverted microscope under 20× lenses (N.A. 0.8) with correction collar for plastic multiwell plates. Thirty to forty random fields were acquired for each well. Neurites were traced and analyzed for total neurite length using NIH ImageJ with the NeuronJ plugin [21]. The number of terminals and the number of branch points were counted manually after tracing. Sholl analysis was performed by using Image J with the Sholl analysis plugin [22]. To avoid any ambiguity, neurons with overlapping neurites were excluded from analysis. The number of independent experiments and the number of TH^+ neurons or TH^- neurons traced and analyzed were listed in each figure legend.

Microtubule stability assay

Free or polymerized tubulin from human iPSC-derived neuronal cultures was extracted using a standard protocol described previously [11]. Briefly, cultures in 24 well plates were washed once at 37°C with 0.5 ml of Buffer A containing 0.1 M MES, pH 6.75, 1 mM $MgSO_4$, 2 mM EGTA, 0.1 mM EDTA, and 4 M glycerol. After the cultures were incubated at 37 °C for 5 min in 600 μl of free tubulin extraction buffer (Buffer A plus 0.1% v/v Triton X-100 and protease inhibitors), the extracts were centrifuged at 37 °C for 2 min at 16,000 × G. The supernatant fractions contained free tubulin extracted from the cytosol. The pellet fraction and lysed cells in the culture dish were dissolved in 600 μl of 25 mM Tris, pH 6.8, plus 0.5% SDS and contained tubulin originally in microtubules. Equal amounts of total proteins from free or polymerized tubulin fractions were analyzed by Western blotting. The intensity of tubulin bands were quantified from at least three different experiments with the

ImageLab software (life science research, Bio-Rad USA). After background subtraction, densities of the bands were quantified against the first lane.

Statistical analyses

All data were expressed as mean ± s.e.m. (standard error of measurement). Unpaired, two-tailed Student's *t*-tests were performed to evaluate whether two groups were significantly different from each other. The number of variables (n) is the total number of neurons analyzed. The values for n and p (in bins of < 0.001, < 0.01 or > 0.05) are included in each figure legend. Values of $p < 0.05$ were considered statistically significant.

Results

Parkin mutations reduce the length and complexity of neuronal processes in iPSC-derived neurons

In the present study, we used the same set of patient-specific iPSCs generated previously [20] to study the impact of parkin on the morphology of midbrain TH^+ neurons and TH^- Neurons. The iPSCs were from two normal subjects (C001 and C002) and two PD patients with different parkin mutations (P001, which has compound heterozygous deletions of exon 3 and exon 5; P002, which has homozygous deletions of exon 3). The same rosette-based method was used to differentiate the iPSCs in parallel to midbrain DA neurons [20]. After about 90 days of differentiation *in vitro*, the midbrain neuronal cultures were fixed and stained with an antibody against tyrosine hydroxylase (TH). We randomly selected 58 TH^+ neurons for each line of iPSC-derived midbrain neuronal cultures from six independent experiments. Representative images showed that TH^+ neurons from the two normal controls (C001 and C002) had much more extensive and elaborate neuronal processes than TH^+ neurons from the two PD patients with parkin mutations (P001 and P002) (Fig. 1A–D). The contours of these TH^+ neurons were traced (Fig. S1A–D) and analyzed by using NIH ImageJ with the NeuronJ plugin [21]. The average total neurite length (Fig. 1E), the average number of terminals (Fig. 1F) and the average number of branch points (Fig. 1G) were significantly reduced in iPSC-derived TH^+ neurons from P001 and P002, compared to the situations in C001 and C002 ($p < 0.001$, n = 58 TH^+ neurons from six independent experiments). Sholl analysis, which measures the complexity of neuronal processes by counting the number of intersections between neurites and a concentric circle at a given radius from the center of the soma [22], showed that neurite complexity of TH^+ neurons was significantly reduced in P001 and P002, in comparison to C001 and C002 ($p < 0.001$, n = 58 TH^+ neurons from six independent experiments) (Fig. 1H). There was no significant difference in the above morphological measurements between the two controls (C001 and C002), or between the two PD patients with parkin mutations (P001 and P002) (Fig. 1E–H).

To examine the situation in TH^- neurons, we infected iPSC-derived midbrain neuronal cultures around 76 days with low titer sindbis virus for palmitoylated GFP (palGFP), which expressed palGFP in well-isolated individual neurons and highlighted the entire neuronal processes [13]. The neuronal cultures were fixed around 90 days and stained for TH to make sure that the $palGFP^+$ neurons that we analyzed were TH^- (Fig. S2A–D). The random and rare transduction of neurons with palGFP ensured that $palGFP^+$ neurons were TH^-, as we

cultured the iPSC-derived neurons at low density to reduce the density of TH^+ neurons. The palGFP$^+$TH$^-$ neurons from C001 and C002 exhibited markedly more extensive and complex neuronal processes than palGFP$^+$TH$^-$ neurons from P001 and P002 (Fig. 1I–L). We traced the contour of these neurons (Fig. S2I–L) and analyzed them with ImageJ/NeuronJ. The average total neurite length (Fig. 1M), the average number of terminals (Fig. 1N) and the average number of branch points (Fig. 1O) were significantly decreased in palGFP$^+$TH$^-$ neurons from P001 and P002, as compared to the situations in C001 and C002 ($p < 0.001$, n = 62 TH^- neurons from six independent experiments). Consistent with these, Sholl analysis showed a significant reduction in neurite complexity (Fig. 1P).

A side-by-side analysis of TH^+ neurons and palGFP$^+$TH$^-$ neurons in the same field (Fig. S2A–L) showed that the average total neurite length was significantly shorter in TH^- neurons than TH^+ neurons derived from the same subject, no matter whether the subject was normal or a PD patient with parkin mutations (Fig. S2M). In contrast, the average number of terminals (Fig. S2N) and the average number of branch points (Fig. S2O) were significantly fewer in TH^- neurons than TH^+ neurons only from normal subjects, but not from PD patients with parkin mutations. Sholl analysis showed that TH^+ neurons were significantly more complex than TH^- neurons from the two normal subjects, while the complexity of TH^+ and TH^- neurons was not significantly different in the two PD patients. It seems that there are intrinsic differences between TH^+ neurons and TH^- neurons in total neurite length and neurite complexity. Parkin mutations abolish the difference in neurite complexity by greatly reducing the complexity of TH^+ neurons to levels comparable to those of TH^- neurons. In contrast, parkin mutations had comparable impacts on total neurite length of TH^+ neurons (~ 1/3 reduction) and TH^- neurons (~ 1/2 reduction) (Fig. S2M).

Overexpression of parkin rescues the morphological defects of parkin-deficient neurons

To ascertain that the reduced neurite length and complexity in PD patients with parkin mutations are caused by parkin mutations, we infected P001 (Fig. 2A–J) and P002 (Fig. 2K–T) midbrain neuronal cultures around 76 days with lentivirus for GFP, FLAG-tagged parkin or its PD linked T240R mutant, which strongly expresses the corresponding transgene in the culture [20]. The midbrain neuronal cultures were fixed around 90 days and stained for TH and GFP or TH and FLAG. In midbrain neuronal cultures from P001, TH^+ neurons expressing wild-type parkin showed longer and more complex neuronal processes (Fig. 2B, E), compared to TH^+ neurons expressing GFP (Fig. 2A, D) or T240R (Fig. 2C, F). The average total neurite length (Fig. 2G), the average number of terminals (Fig. 2H) and the average number of branch points (Fig. 2I) were significantly increased by exogenously expressed parkin, but not by its T240R mutant or GFP. Sholl analysis showed that overexpression of parkin, but not its T240R mutant or GFP, significantly increased the complexity of neuronal processes (Fig. 2J). We found that the overexpression of parkin, but not T240R or GFP, achieved similar rescue in TH^+ neurons derived from P002 (Fig. 2K–T). There was no significant difference in the degree of rescue between P001 and P002 (Fig. S3A–F).

When we analyzed TH^- neurons in the same set of midbrain neuronal cultures differentiated from P001 (Fig. 3A–J) and P002 (Fig. 3K–T) iPSCs, we found that the overexpression of

parkin (Fig. 3B, E, L, O), but not T240R (Fig. 3C, F, M, P) or GFP (Fig. 3A, D, K, N), significantly increased the average total neurite length (Fig. 3G, Q), the average number of terminals (Fig. 3H, R), the average number of branch points (Fig. 3I, S), and neurite complexity as measured by Sholl analysis (Fig. 3J, T). For TH^- neurons, there was no significant difference between P001 and P002 in the rescue by parkin or the lack thereof by GFP or T240R (Fig. S3G–L).

To substantiate the effect of parkin expression on neuronal morphology, we infected C001 and C002 neurons around 76 days with lentivirus expressing GFP, FLAG-tagged parkin or FLAG-tagged T240R mutant parkin. The neuronal cultures were fixed around 90 days and stained for TH and GFP or TH and FLAG to identify TH^+ or TH^- neurons expressing various constructs (Fig. S4A–C for C001 and Fig. S4R–T for C002). Morphological analysis of the traced TH^+ neurons (Fig. S4D–J) and TH^- neurons (Fig. 4K–Q) from C001 and C002 (Fig. S4U-AA for TH^+ neurons, Fig. S4AB–AH for TH^- neurons) showed that overexpression of wild-type parkin, but not its T240R mutant or GFP, significantly increased total neurite length (Fig. S4G), the number of terminals (Fig. S4H), the number of branch points (Fig. S4I) and complexity of neuronal processes as measured by Sholl analysis (Fig. S4J) for TH^+ neurons and for TH^- neurons (Fig. S4N–Q) from C001. The same is also true for C002 neurons (Fig. S4X-AA for TH^+ neurons and Fig. S4AE–AH) for TH^- neurons).

Parkin mutations reduce microtubule stability in iPSC-derived neurons

Our previous studies have shown that parkin stabilizes microtubules [9,10]. To test whether microtubule stability is involved in the significant differences in neurite length and complexity between normal and parkin-deficient iPSC-derived neurons, we measured the amount of free tubulin in cytosolic fractions and polymerized tubulin (i.e. in microtubules) in pellet fractions in midbrain neuronal cultures treated without or with colchicine (Col, 10 μm for 30 min). Without any treatment, there was significantly more free tubulin in P001 and P002, as compared to that in C001 and C002 (Fig. 4A, C). After colchicine treatment, the amount of free tubulin was also much more in P001 and P002 than that in C001 and C002 (Fig. 4A, C). Consistent with these, the amount of polymerized tubulin in pellet fractions was significantly less in P001 and P002, compared to that in C001 and C002, under control condition or with colchicine treatment (Fig. 4B, D).

Overexpression of parkin stabilizes microtubules in iPSC-derived neurons

The above results suggest that parkin mutations in P001 and P002 iPSC-derived midbrain neurons render microtubules less stable. To substantiate this finding, we infected P001 and P002 midbrain neuronal cultures around day 76 with lentivirus expressing GFP or FLAG-tagged parkin or its PD linked T240R mutant [20]. The amount of free or polymerized tubulin was measured by Western blotting at day 90. In the absence of any drug treatment, overexpression of wild-type parkin, but not its T240R mutant or GFP, significantly decreased the amount of free tubulin in cytosolic fractions in P001 and P002 midbrain neuronal cultures. The effects remained the same with colchicine treatment (Fig. 5A, C, E). The amount of polymerized tubulin in pellet fractions was significantly increased by parkin,

but not its T240R mutant or GFP, in P001 and P002 midbrain neuronal cultures without or with colchicine treatment (Fig. 5B, D, F).

To substantiate the microtubule-stabilizing effect of parkin, we also infected C001 and C002 midbrain neuronal cultures around day 76 with lentivirus expressing GFP, FLAG-tagged parkin or FLAG-tagged T240R mutant parkin [20]. The amount of free or polymerized tubulin was measured by Western blotting at day 90. In the absence of any drug treatment, overexpression of wild-type parkin, but not its T240R mutant or GFP, significantly decreased the amount of free tubulin in cytosolic fractions in C001 and C002 midbrain neuronal cultures (Fig. S5A, C, E). The effects remained the same with colchicine treatment (Fig. S5A, C, E). The amount of polymerized tubulin in pellet fractions was significantly increased by parkin, but not its T240R mutant or GFP, in C001 and C002 midbrain neuronal cultures treated with vehicle or colchicine (Fig. S5B, D, F).

Microtubule depolymerization reduces neurite length and complexity in control neurons

Our results showed that parkin stabilized microtubules and increased neurite length and complexity. To explore the link between microtubule stability and neuronal morphology, we treated C001 and C002 neurons around 60 days of differentiation with vehicle (i.e. differentiation media) or 1 nM colchicine for 14 days. The neuronal cultures were maintained in differentiation media for two more weeks before being stained with anti-TH around 90 days (Fig. 6A–D for representative morphology of TH^+ neurons and Fig. 6I–L for representative morphology of TH^- neurons). The very low dose chronic treatment of the microtubule-depolymerizing agent colchicine did not cause any significant cell death (data not shown). However, colchicine treatment significantly decreased total neurite length (Fig. 6E), the number of terminals (Fig. 6F), the number of branch points (Fig. 6G) and neurite complexity as measured by Sholl analysis (Fig. 6H) for TH^+ neurons from C001 and C002, as well as for TH^- neurons differentiated from both iPSCs (Fig. 6M–P). Thus, the microtubule-depolymerizing agent colchicine mimicked the effect of parkin mutations on neuronal morphology.

Microtubule stabilization increases neurite length and complexity in parkin-deficient neurons

To substantiate the results above, we treated P001 and P002 neurons around 60 days of differentiation with vehicle (i.e. differentiation media) or 1 nM taxol for 14 days. The neuronal cultures were maintained in differentiation media for two more weeks before being stained with anti-TH around 90 days (Fig. 7A–D for representative morphology of TH^+ neurons and Fig. 7I–L for representative morphology of TH^- neurons). The very low dose chronic treatment of the microtubule-stabilizing agent taxol did not cause any significant cell death (data not shown). However, taxol treatment significantly increased total neurite length (Fig. 7E), the number of terminals (Fig. 7F), the number of branch points (Fig. 7G) and neurite complexity as measured by Sholl analysis (Fig. 7H) for TH^+ neurons from P001 and P002, as well as for TH^- neuron differentiated from both iPSCs (Fig. 7M–P). Thus, the microtubule-stabilizing agent taxol mimicked the effect of parkin overexpression by restoring neuronal morphology in parkin-deficient neurons.

Discussion

In this study, we found that parkin mutations significantly reduced the length and complexity of neuronal processes in patient-specific iPSC-derived midbrain neurons. The effect was not specific to TH^+ neurons; TH^- neurons were also affected by parkin mutations (Fig. 1). However, parkin mutations had a stronger impact on the complexity of TH^+ neurons than TH^- neurons. The number of terminals, the number of branch points and the number of intersections in Sholl analysis in TH^+ neurons were markedly reduced by parkin mutations so that there was no significant difference between TH^+ and TH^- neurons (Fig. S2N–P). This is in sharp contrast to the situation in normal controls, which exhibited significant difference in neurite complexity between TH^+ neurons and TH^- neurons (Fig. S2N–P). The greater loss of neurite complexity in iPSC-derived TH^+ neurons from PD patients with parkin mutations reflects the increased vulnerability of nigral DA neurons vis-à-vis other types of neurons in Parkinson's disease [23,24]. Patient-specific iPSC-derived midbrain DA neurons thus offer a useful model to study such vulnerability [25–27].

One unique vulnerability of nigral DA neurons appears to be their microtubule network [28–31]. Midbrain DA neurons are particularly sensitive to microtubule-depolymerizing agents, including the environmental PD toxin rotenone [11,32,33]. Our previous studies showed that overexpression of parkin protects against these microtubule-depolymerizing toxins by stabilizing microtubules and thus attenuating the activation of MAP kinases induced by microtubule-depolymerization [12]. In the present study, we found that parkin mutations significantly decreased microtubule stability in iPSC-derived midbrain neurons (Fig. 4). Overexpression of parkin, but not its PD-linked T240R mutant or GFP, significantly increased microtubule stability (Fig. 5) and rescued the morphological defects in parkin-deficient neurons (Fig. 2 and Fig. 3). In fact, the effects of parkin on microtubule stability (Fig. S5) and neuronal morphology (Fig. S4) were similarly seen when parkin was overexpressed in iPSC-derived neurons from normal subjects.

To strengthen the link between the two effects of parkin – microtubule stabilization and maintenance of neuronal morphology, we showed that the microtubule-depolymerizing agent colchicine mimicked the effect of parkin mutations by decreasing neurite length and complexity in control neurons (Fig. 6), while the microtubule-stabilizing drug taxol mimicked the effect of parkin overexpression by enhancing neurite length and complexity in patient neurons (Fig. 7). Together, our results suggest that parkin maintains the extensive and elaborate neuronal processes by stabilizing microtubules. Mutations of parkin disrupt this critical function and may reduce the ability of nigral DA neurons to maintain widespread connections to striatal neurons.

Conclusion

Results from the present study demonstrate that parkin stabilizes microtubules to maintain the length and complexity of neuronal processes. This function would be particularly important to the survival and function of nigral DA neurons, which have massive axon arborization [13]. Mutations of parkin disrupt this important function and thus render the neurons highly vulnerable in Parkinson's disease.

Supplementary Material

Refer to Web version on PubMed Central for supplementary material.

Acknowledgments

The work was supported by the Michael J. Fox Foundation for Parkinson's Research, National Key Basic Research Program of China (2011CB504100), NYSTEM contracts C028129 and C026714, NIH grant NS061856, SUNY REACH, and Department of Veterans Affairs Merit Award I01BX002452. We would like to thank Dr. Takahiro Furuta at Kyoto University for providing the pSinRep5-palGFP construct [13].

References

1. Lang AE, Lozano AM. Parkinson's disease. First of two parts. N Engl J Med. 1998; 339:1044–1053. [PubMed: 9761807]
2. Kitada T, Asakawa S, Hattori N, et al. Mutations in the parkin gene cause autosomal recessive juvenile parkinsonism. Nature. 1998; 392:605–608. [PubMed: 9560156]
3. Nuytemans K, Theuns J, Cruts M, et al. Genetic etiology of Parkinson disease associated with mutations in the SNCA, PARK2, PINK1, PARK7, and LRRK2 genes: a mutation update. Hum Mutat. 2010; 31:763–780. [PubMed: 20506312]
4. Shimura H, Hattori N, Kubo S, et al. Familial Parkinson disease gene product, parkin, is a ubiquitin-protein ligase. Nat Genet. 2000 Jul; 25(3):302–5. [PubMed: 10888878]
5. Narendra D, Tanaka A, Suen DF, et al. Parkin is recruited selectively to impaired mitochondria and promotes their autophagy. J Cell Biol. 2008; 183:795–803. [PubMed: 19029340]
6. Kim KY, Stevens MV, Akter MH, et al. Parkin is a lipid-responsive regulator of fat uptake in mice and mutant human cells. J Clin Invest. 2011; 121:3701–3712. [PubMed: 21865652]
7. Manzanillo PS, Ayres JS, Watson RO, et al. The ubiquitin ligase parkin mediates resistance to intracellular pathogens. Nature. 2013; 501:512–516. [PubMed: 24005326]
8. Chen Y, Dorn GW. PINK1-phosphorylated mitofusin 2 is a Parkin receptor for culling damaged mitochondria. Science. 2013; 340:471–475. [PubMed: 23620051]
9. Ren Y, Zhao JH, Feng J. Parkin binds to alpha/beta tubulin and increases their ubiquitination and degradation. Journal of Neuroscience. 2003; 23:3316–3324. [PubMed: 12716939]
10. Yang F, Jiang Q, Zhao J, et al. Parkin Stabilizes Microtubules through Strong Binding Mediated by Three Independent Domains. J Biol Chem. 2005; 280:17154–17162. [PubMed: 15737990]
11. Ren Y, Liu W, Jiang H, et al. Selective vulnerability of dopaminergic neurons to microtubule depolymerization. J Biol Chem. 2005; 280:34105–34112. [PubMed: 16091364]
12. Ren Y, Jiang H, Yang F, et al. Parkin protects dopaminergic neurons against microtubule-depolymerizing toxins by attenuating microtubule-associated protein kinase activation. J Biol Chem. 2009; 284:4009–4017. [PubMed: 19074146]
13. Matsuda W, Furuta T, Nakamura KC, et al. Single nigrostriatal dopaminergic neurons form widely spread and highly dense axonal arborizations in the neostriatum. J Neurosci. 2009; 29:444–453. [PubMed: 19144844]
14. Pissadaki EK, Bolam JP. The energy cost of action potential propagation in dopamine neurons: clues to susceptibility in Parkinson's disease. Front Comput Neurosci. 2013; 7:13. [PubMed: 23515615]
15. Bolam JP, Pissadaki EK. Living on the edge with too many mouths to feed: why dopamine neurons die. Mov Disord. 2012; 27:1478–1483. [PubMed: 23008164]
16. Iseki E, Kato M, Marui W, et al. A neuropathological study of the disturbance of the nigro-amygdaloid connections in brains from patients with dementia with Lewy bodies. J Neurol Sci. 2001; 185:129–134. [PubMed: 11311294]
17. Raff MC, Whitmore AV, Finn JT. Axonal self-destruction and neurodegeneration. Science. 2002; 296:868–871. [PubMed: 11988563]
18. Dawson TM, Ko HS, Dawson VL. Genetic animal models of Parkinson's disease. Neuron. 2010; 66:646–661. [PubMed: 20547124]

19. Perez FA, Palmiter RD. Parkin-deficient mice are not a robust model of parkinsonism. Proc Natl Acad Sci U S A. 2005; 102:2174–2179. [PubMed: 15684050]
20. Jiang H, Ren Y, Yuen EY, et al. Parkin controls dopamine utilization in human midbrain dopaminergic neurons derived from induced pluripotent stem cells. Nat Commun. 2012; 3:668. [PubMed: 22314364]
21. Meijering E, Jacob M, Sarria JC, et al. Design and validation of a tool for neurite tracing and analysis in fluorescence microscopy images. Cytometry A. 2004; 58:167–176. [PubMed: 15057970]
22. Kumamoto N, Gu Y, Wang J, et al. A role for primary cilia in glutamatergic synaptic integration of adult-born neurons. Nat Neurosci. 2012; 15:399–405. S1. [PubMed: 22306608]
23. Hirsch E, Graybiel AM, Agid YA. Melanized dopaminergic neurons are differentially susceptible to degeneration in Parkinson's disease. Nature. 1988; 334:345–348. [PubMed: 2899295]
24. Braak H, Braak E. Pathoanatomy of Parkinson's disease. J Neurol. 2000; 247(Suppl 2):II3–10. [PubMed: 10991663]
25. Bellin M, Marchetto MC, Gage FH, et al. Induced pluripotent stem cells: the new patient? Nat Rev Mol Cell Biol. 2012; 13:713–726. [PubMed: 23034453]
26. Pu J, Jiang H, Zhang B, et al. Redefining Parkinson's disease research using induced pluripotent stem cells. Curr Neurol Neurosci Rep. 2012; 12:392–398. [PubMed: 22622410]
27. Badger JL, Cordero-Llana O, Hartfield EM, et al. Parkinson's disease in a dish - Using stem cells as a molecular tool. Neuropharmacology. 2014; 76(Pt A):88–96. [PubMed: 24035919]
28. Feng J. Microtubule: a common target for parkin and Parkinson's disease toxins. Neuroscientist. 2006; 12:469–476. [PubMed: 17079513]
29. Dickson DW. Parkinson's disease and parkinsonism: neuropathology. Cold Spring Harb Perspect Med. 2012; 2
30. Law BM, Spain VA, Leinster VH, et al. A direct interaction between Leucine-rich Repeat Kinase 2 and specific beta-tubulin isoforms regulates tubulin acetylation. J Biol Chem. 2013
31. Sheng C, Heng X, Zhang G, et al. DJ-1 deficiency perturbs microtubule dynamics and impairs striatal neurite outgrowth. Neurobiol Aging. 2013; 34:489–498. [PubMed: 22609282]
32. Choi WS, Kruse SE, Palmiter RD, et al. Mitochondrial complex I inhibition is not required for dopaminergic neuron death induced by rotenone, MPP+, or paraquat. Proc Natl Acad Sci U S A. 2008; 105:15136–15141. [PubMed: 18812510]
33. Choi WS, Palmiter RD, Xia Z. Loss of mitochondrial complex I activity potentiates dopamine neuron death induced by microtubule dysfunction in a Parkinson's disease model. J Cell Biol. 2011; 192:873–882. [PubMed: 21383081]

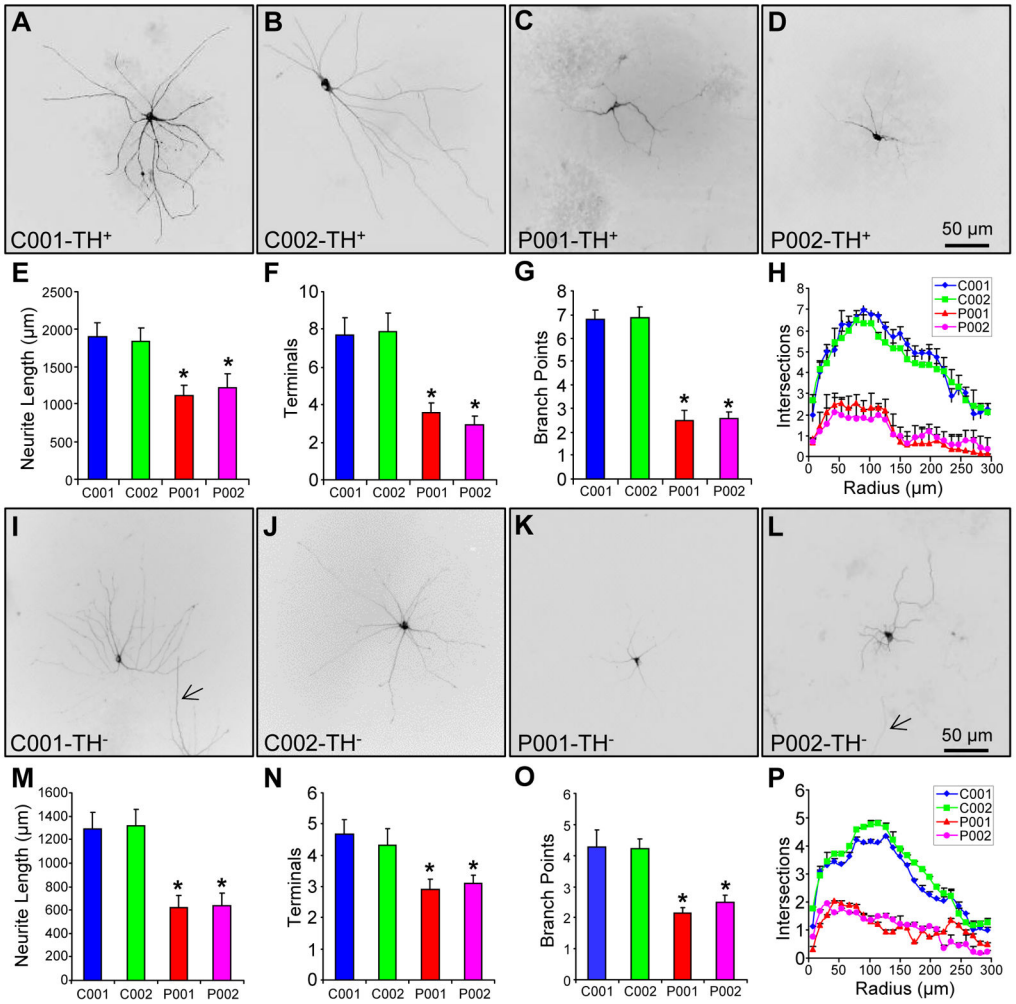

Figure 1.

Morphology of iPSC-derived neurons from normal subjects and PD patients with parkin mutations. **(A–H)** Representative images of iPSC-derived TH^+ neurons from two normal controls (A, B) and two PD patients with different parkin mutations (C, D). Total neurite length per neuron (E), number of terminals per neuron (F), number of branch points per neuron (G) and Sholl analysis (H) were quantified. **(I–P)** Representative images of iPSC-derived TH^- neurons (highlighted by low titer palGFP sindbis virus) from the two normal controls (I, J) and the two PD patients with parkin mutations (K, L), as well as quantification of total neurite length per neuron (M), number of terminals per neuron (N), number of branch points per neuron (O) and Sholl analysis (P). *, $p < 0.001$, vs. C001 or C002, n = 58 for TH^+ neurons for each line of iPSC in E–H and n = 62 for TH^- neurons for each line of iPSC in M–P, all from 6 independent experiments. Bar, 50μm. Arrow, process from another neuron.

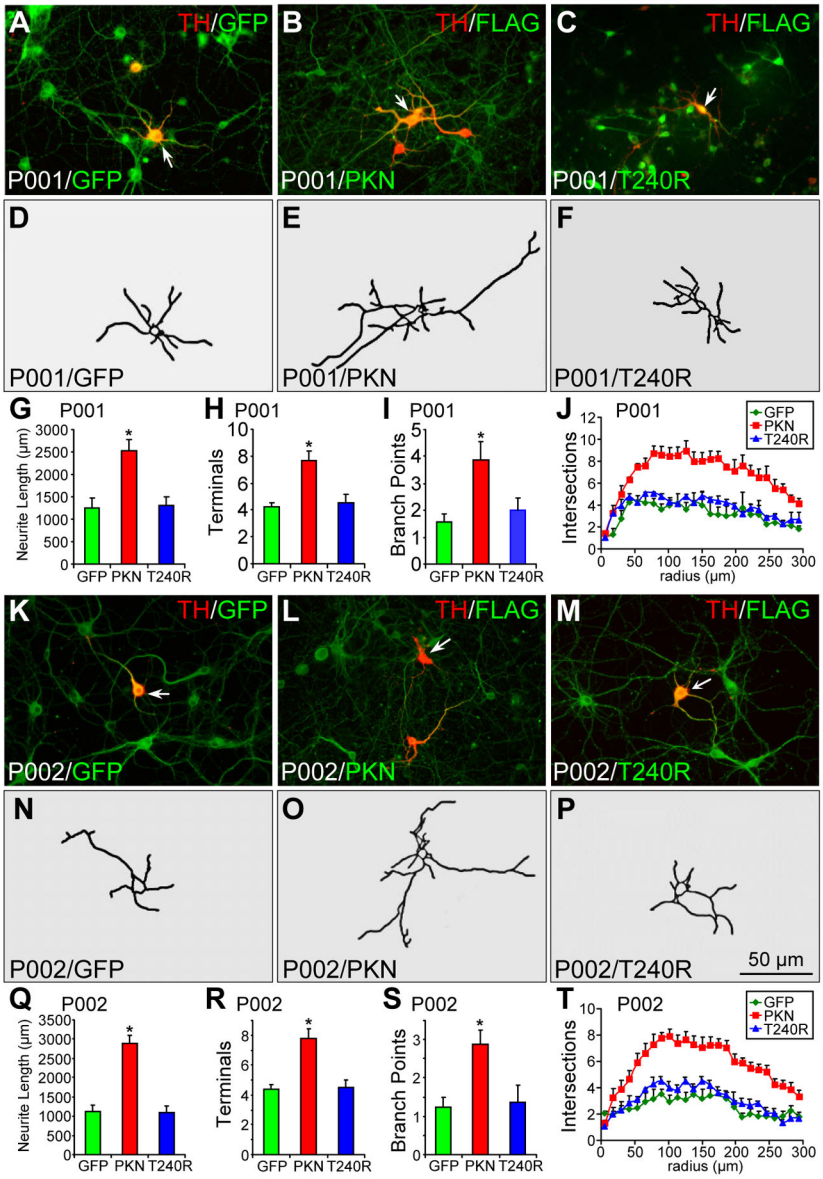

Figure 2.

Morphology of parkin-deficient TH$^+$ neurons infected with lentivirus expressing GFP, wild-type or mutant parkin. **(A–J)** P001 iPSC-derived neurons were infected with lentivirus expressing GFP (A), FLAG-parkin (B) or FLAG-T240R mutant parkin (C) and co-stained for TH and GFP (A) or TH and FLAG (B, C). Contour of TH$^+$ neurons identified by the arrow was traced in (D–F). Total neurite length per neuron (G), number of terminals per neuron (H), number of branch points per neuron (I) and Sholl analysis (J) were quantified. **(K–T)** P002 iPSC-derived neurons were infected with lentivirus expressing GFP (K), FLAG-parkin (L) or FLAG-T240R mutant parkin (M) and co-stained for TH and GFP (K) or TH and FLAG (L, M). Contour of TH$^+$ neurons identified by the arrow was traced in (N–P). Total neurite length per neuron (Q), number of terminals per neuron (R), number of branch points per neuron (S) and Sholl analysis (T) were quantified. Arrows, TH$^+$ neurons

that were traced. Bar, 50 μm. *, $p < 0.001$, vs. GFP, n = 45 TH^+ neurons for each derivative line of P001 neurons in G–J and n = 47 TH^+ neurons for each derivative line of P002 neurons in Q–T, all from three independent experiments.

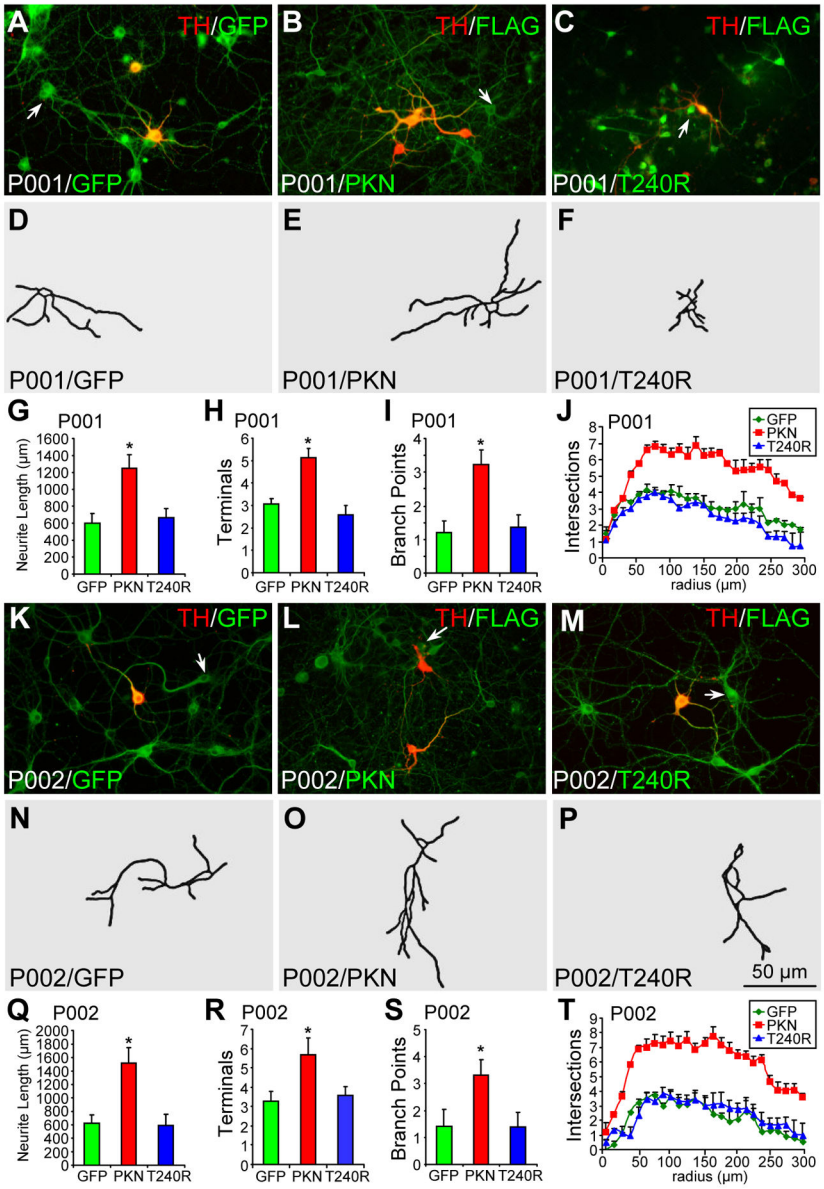

Figure 3.

Morphology of parkin-deficient TH⁻ neurons infected with lentivirus expressing GFP, wild-type or mutant parkin. **(A–J)** P001 iPSC-derived neurons were infected with lentivirus expressing GFP (A), FLAG-parkin (B, PKN) or FLAG-T240R mutant parkin (C, T240R) and co-stained for TH and GFP (A) or TH and FLAG (B, C). Contour of TH⁻ neurons identified by the arrow was traced in (D–F). Total neurite length per neuron (G), number of terminals per neuron (H), number of branch points per neuron (I) and Sholl analysis (J) were quantified. **(K–T)** P002 iPSC-derived neurons were infected with lentivirus expressing GFP (K), FLAG-parkin (L, PKN) or FLAG-T240R mutant parkin (M, T240R) and co-stained for TH and GFP (K) or TH and FLAG (L, M). Contour of TH⁻ neurons identified by the arrow was traced in (N–P). Total neurite length per neuron (Q), number of terminals per neuron (R), number of branch points per neuron (S) and Sholl analysis (T) were quantified. Arrows,

TH^- neurons that were traced. Bar, 50 μm. *, $p < 0.001$, vs. GFP, n = 46 TH^- neurons for each derivative line of P001 neurons in G–J and n = 47 TH^- neurons for each derivative line of P002 neurons in Q–T, all from three independent experiments.

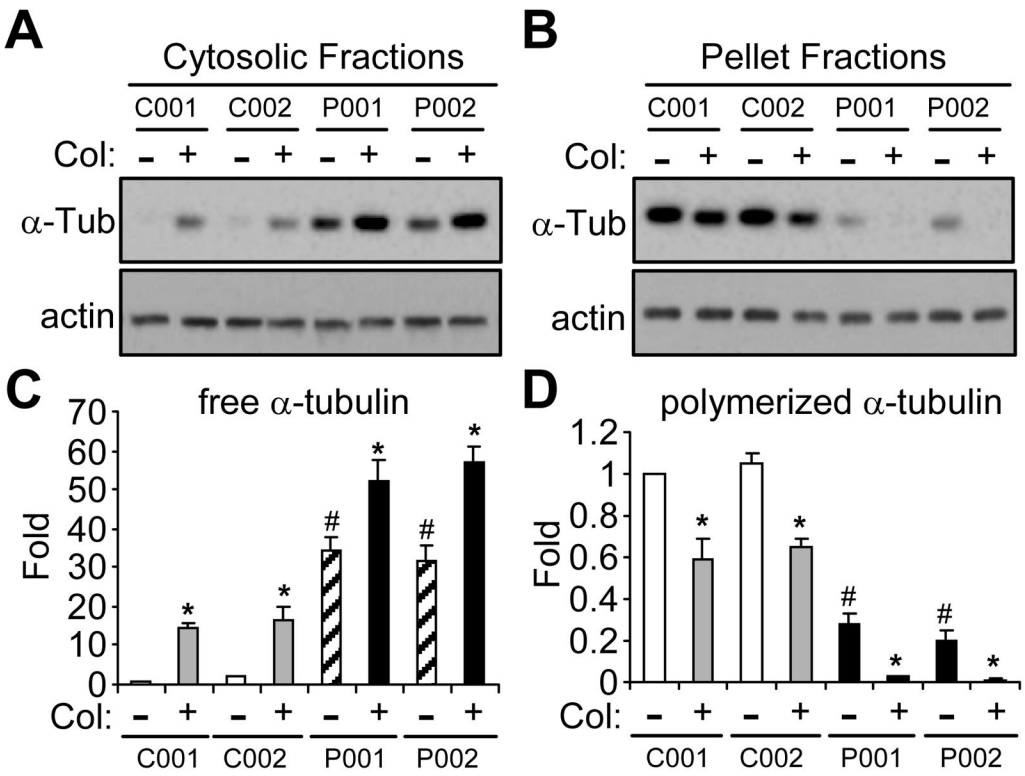

Figure 4.

Microtubule stability in iPSC-derived neurons from normal subjects or PD patients with parkin mutation. **(A–D)** iPSC-derived neuronal cultures from two normal subjects (C001 and C002) and two PD patients with different parkin mutations (P001 and P002) were treated without or with colchicine (Col, 10 μm for 30 min). Cytosolic (A) or pellet (B) fractions of these cells were blotted with antibodies against α-tubulin or actin. The amount of free tubulin in cytosolic fractions (C) and polymerized tubulin in pellet fractions (D) were quantified by normalizing against the amount of α-tubulin in the first lane. *, $p < 0.001$, vs. the preceding bar; #, $p < 0.001$, vs. C001 or C002 without colchicine treatment, n = 3 independent experiments.

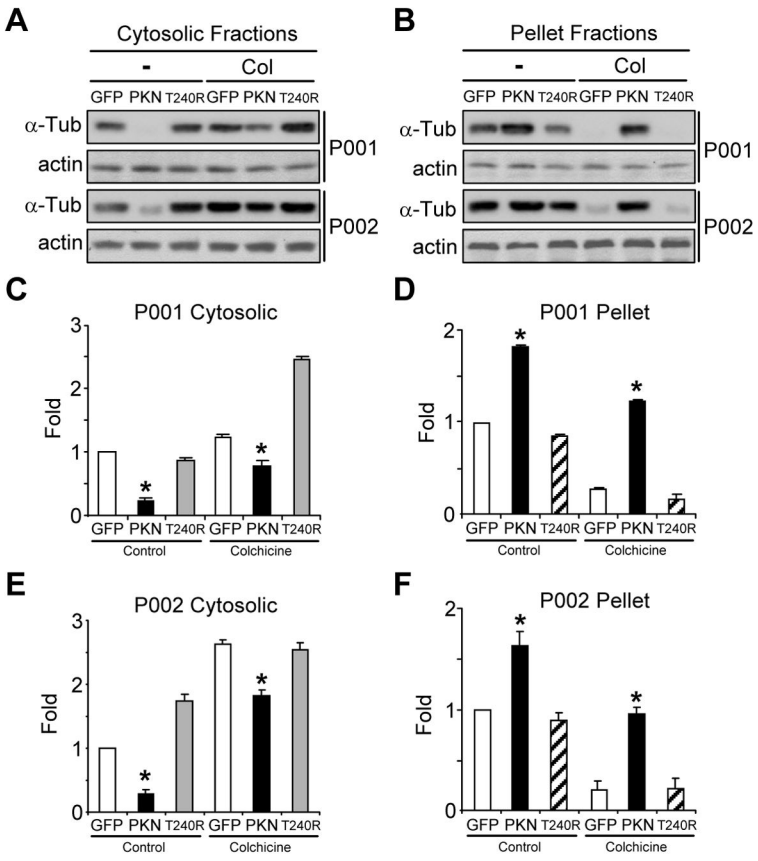

Figure 5.

Microtubule stability in parkin-deficient neurons infected with lentiviruses expressing GFP, wild-type or mutant parkin. **(A–F)** iPSC-derived neuronal cultures from two PD patients with parkin mutations (P001 and P002) were infected with lentiviruses expressing GFP, wild-type parkin (PKN) or its PD-linked T240R mutant (T240R). After colchicine (Col) treatment (10 μM for 30 min), cytosolic fractions (A) and pellet fractions (B) were blotted with antibodies against α-tubulin or actin. The amount of free tubulin in cytosolic fractions (C, E) and polymerized tubulin in pellet fractions (D, F) were quantified by normalizing against the amount of α-tubulin in the first lane of P001 (C, D) or P002 (E, F), respectively. *, $p < 0.001$, vs. the preceding bar, n = 3 independent experiments.

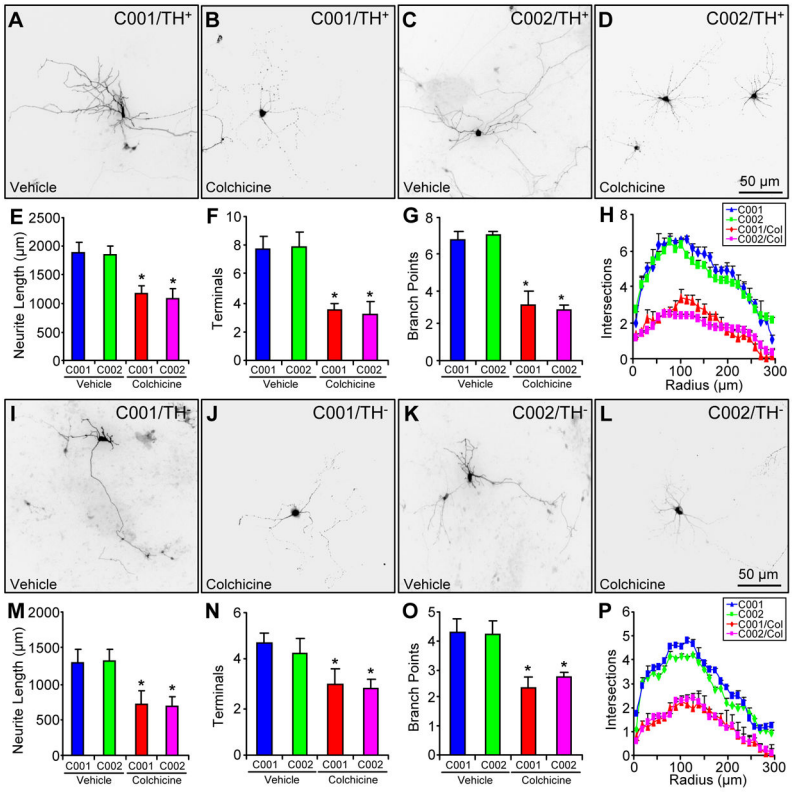

Figure 6.

The impact of colchicine on the morphology of control neurons. (**A–H**) Representative morphology of C001 (A, B) or C002 (C, D) TH^+ neurons treated with vehicle (A, C) or colchicine (1 nM for 14 days) (B, D) and quantification of their total neurite length (E), number of terminals (F), number of branch points (G) and Sholl analysis (H). (**I–P**) Representative morphology of C001 (I, J) or C002 (K, L) TH^- neurons treated with vehicle (I, K) or colchicine (1 nM for 14 days) (J, L) and quantification of their total neurite length (M), number of terminals (N), number of branch points (O) and Sholl analysis (P). *, $p < 0.001$, vs. vehicle-treated C001 or C002, n = 52 TH^+ neurons and n = 54 TH^- neurons for each condition of C001 or C002 neurons, all from three independent experiments.

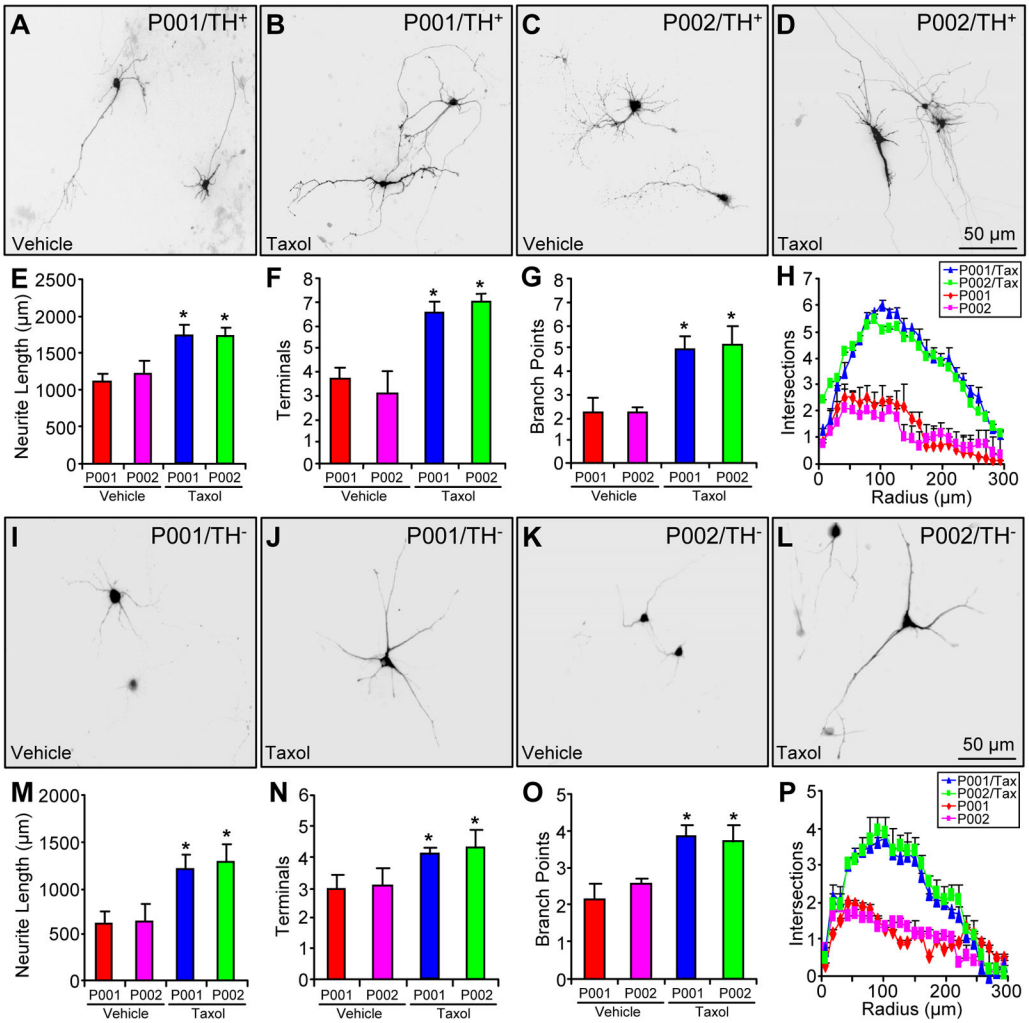

Figure 7.

The impact of taxol on the morphology of parkin-deficient neurons. (**A–H**) Representative morphology of P001 (A, B) or P002 (C, D) TH^+ neurons treated with vehicle (A, C) or taxol (1 nM for 14 days) (B, D) and quantification of their total neurite length (E), number of terminals (F), number of branch points (G) and Sholl analysis (H). (**I–P**) Representative morphology of P001 (I, J) or P002 (K, L) TH^- neurons treated with vehicle (I, K) or taxol (1 nM for 14 days) (J, L) and quantification of their total neurite length (M), number of terminals (N), number of branch points (O) and Sholl analysis (P). *, $p < 0.001$, vs. vehicle-treated P001 or P002, n = 52 TH^+ neurons and n = 54 TH^- neurons for each condition of P001 or P002 neurons, all from three independent experiments.